International Journal of System Dynamics Applications
Volume 10 • Issue 4

Sensorless Control of Induction Motor Based on Differential Flatness Theory and Reduced MRAS Observer

Laggoun Louanasse, University of Khenchela, Algeria
Beddiaf Yassine, University of Khenchela, Algeria*

ABSTRACT

In this paper, the authors propose a hybrid sensorless control method of IM. This method consists of using the differential flatness theory and reduced MRAS observer. The control design proceeds by showing that each input of the motor model stands for a differentially flat system, where the flat output is chosen to be the associated state variable. Next, for each regulation loop a virtual control input is computed that can invert the loop's dynamics and can eliminate the system's tracking error. The reduced MRAS observer is used to estimate the rotor speed and flux. Simulation and experimental results are presented to illustrate the effectiveness of the proposed approach for sensorless control of the induction motor.

KEYWORDS

Differential Flatness Theory, Induction Motor, Reduced MRAS Observer, Sensorless Vector Control

1. INTRODUCTION

The sensorless control of induction machine is a very broad area of research, and for that, a very large number of researches who have contributed to this. However, many problems related to parametric variations and the mechanical speed sensor still persist. Vector control and especially sensorless control can lose its performance because of these problems, because generally this kind of control depends on the stator and rotor time constant (Armando, Boglietti, Musumeci, & Rubino, 2021) (Savarapu & Narri), in this context, several strategies have been proposed in the literature to realize the sensorless control of this machine. A large part of the proposed methods is based on observers depending on the model of the asynchronous machine (Vasu, Thalluru, & Kumar, 2021), (Adamczyk & Orlowska-Kowalska, 2021; Al-Rouh, 2004; Comanescu, 2016; De Wit, Ortega, & Mareels, 1996; Manceur, 2012; Morand, 2005; Beddiaf Yassine, Fatiha, & Chrifi-Alaoui; Zbede, Gadoue, & Atkinson, 2016). Other research is on the contribution of artificial intelligence to improve sensorless control of the machine(Abdollahi, 2021) (Chang, Espinosa-Perez, Mendes, & Ortega, 2000; De Doncker & Novotny, 1994; Hussein, Ammar, & Hassan, 2017; Ismail, 2012; Lorenz, Lipo, & Novotny, 1994). In paper (Enany, Wahba, & Hassan, 2014) the author proposes a new technique to model the stator winding, for using to validate a remote and sensorless stator winding temperature estimation technique. (Salima, Loubna, & Riad, 2018) present a global stability and robust nonlinear controller applied to induction motor. (Mustafa, Nikolakopoulos, & Gustafsson, 2014) present a fault classification algorithm based on a robust linear discrimination scheme, this technique is applied to detect of two kinds of Induction

DOI: 10.4018/IJSDA.295091 *Corresponding Author

motor faults (broken rotor bar and short circuit in stator winding) in (Nazemi, Gallehdar, Haghjoo, & Cruz, 2021) the authors present a new sensitive fault detection criterion is proposed, based on the stationary wavelet transform (SWT) decomposition components of the stator currents in objective is, the detection of stator faults in line-connected and inverter-fed motors . Despite all these studies, we didn't manage to replace the speed sensor exactly mainly during in the load's application.

In this context and in order to correct some problems related to the vector control, we propose the using of flatness theory in order to end up with a cascade (hybrid) vector control.

It should be noted that the flatness theory is a more or less recent notion in automatic that was proposed from (Dannehl & Fuchs, 2006; Fliess, Lévine, Martin, & Rouchon, 1995) and (Fliess, Lévine, Martin, & Rouchon, 1999). This concept makes it possible to control of dynamic system. The concept of flatness theory is based on the highlighting of flat outlets (Ha & Quang, 2019, 2020). The first step of control by the flatness method is to generate a desired trajectory that takes into account the model of system. In the second step, this control requires the design of a loopback control allowing the continuation of this trajectory.

The proposed control is verified and validated by simulation and by experimental testing.

2. DIFFERENTIAL FLATNESS THEORY

Consider a dynamic system defined by the following state equation:

$$\frac{dX}{dt} = f\left(X,U\right) \tag{1}$$

With state vector $X\left(t\right) \in \mathcal{R}^n$ input vector $U\left(t\right) \in \mathcal{R}^m$ where f is a regular vector field, is differentially flat if there exists a vector $y\left(t\right) \in \mathcal{R}^m$ in the form

$$y\left(t\right) = \mathcal{A}\left(X\left(t\right),U\left(t\right),\dot{U}\left(t\right),.....,U^q\left(t\right)\right) \tag{2}$$

Such that

$$X\left(t\right) = \mathcal{B}\left(y\left(t\right),\dot{y}\left(t\right),.....,y^r\left(t\right)\right) \tag{3}$$

$$U\left(t\right) = \mathcal{C}\left(y\left(t\right)\dot{y}\left(t\right),.....,y^{r+1}\left(t\right)\right) \tag{4}$$

Where $\mathcal{A}$, $\mathcal{B}$ and $\mathcal{C}$ are smooth functions. Therefore that the new systems description is given by the m algebraic variables $y\left(t\right)$.

Since the components of $y\left(t\right)$ are differentially independent, the output plate groups all the free variables of the system. But one can also say, through the equation (2), which does not depend on the state and the control, what makes an endogenous variable system, for example in the state of an observer who is an exogenous variable of the system.

Moreover, the notion of differential equivalence in (Fliess et al., 1999) sense shows it well, the number of components of $y\left(t\right)$ is given by that of the command that is to say dim $y\left(t\right) = dimU\left(t\right)$.

This property allows knowing a priori the number of free variables that must be found on a model to highlight its flatness. To clarify the notion of flatness theory, we consider the following example:

$$\begin{cases} \dot{X}_1(t) = X_2(t) \\ \dot{X}_2(t) = U(t) \end{cases} \tag{5}$$

we define the following variables
$y(t) = X_2(t)$ And $U(t) = \dot{y}(t)$
So, we deduce

$$X_1(t) = X_1(t_0) + \int_{t_0}^{t} y(\tau)\, d\tau \tag{6}$$

So y (t) cannot be considered a flat output because the relation (2) is not verified.
If now, we defines, $y(t) = \ddot{X}_1(t)$ then:

$X_2(t) = \dot{y}(t)$ And $U(t) = \ddot{y}(t)$

In this case, we can say that $X_1(t)$ is a flat output, therefore this system is flat and flat output $y(t) = X_1(t)$.

2.1 Control Law Synthesis Methodology for Flat Systems

The synthesis of a control law for a flat system requires a strategy based on the following approaches:

- Generation of the trajectories of the reference flat output y_{ref}
- Generation of the corresponding reference input u_{ref} trajectory (controls).
- Synthesis of a strategy of stabilization of the control around the planned reference trajectories.

2.2 Trajectory Planning

From the relation (4), if we wish to obtain for the flat system (1), the trajectory: $z_d(t)$ for a time t from t_0 to t_f, it suffices to impose, on the same time segment, the following open-loop control:

$$U_d(t) = B\left(z_d(t), \dot{z}_d(t), \ldots\ldots\ldots\ldots z_d^{(\beta)}(t)\right) \tag{7}$$

In the hypothesis of a perfect model, we will then have, for t from t_0 to t_f, $y(t) = y_d(t)$, therefore:

$$X(t) = X_d(t) = A\left(z_d(t), \dot{z}_d(t), \ldots\ldots\ldots\ldots z_d^{(\alpha)}(t)\right) \tag{8}$$

$$y(t) = y_d(t) = C\left(z_d(t), \dot{z}_d(t), \ldots\ldots\ldots\ldots z_d^{(\gamma)}(t)\right) \tag{9}$$

2.3 Stabilization around Reference Trajectories

A control developed from the flatness concept is established and defined for an open-loop trajectory tracking. The perfect chase is ensured when the system is not disturbed. However, non-linear physical systems are subjected on the one hand to disturbances inherent to their working context, and on the other hand to uncertainties about the parameters. It is therefore necessary to provide a solution to stabilize the system around the trajectories if they are disturbed. Figure 1 illustrates the principle of stabilization of the control by insertion of feedback loop.

Figure 1. Bloc diagram of stabilization.

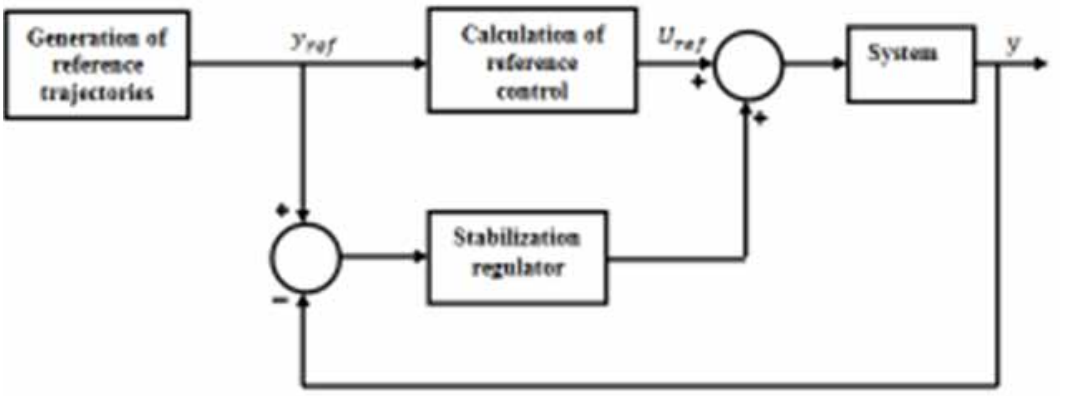

3. FLATNESS CONTROL OF IM

In this section, we demonstrate the flatness of IM mathematical model then the design the proposed control.

3.1 Analysis of the Flatness of IM Model

The mathematical model of IM in stationary reference frame is given by the following equations:

$$\bar{V}_s = R_s \bar{i}_s + \frac{d}{dt}\bar{\varphi}_s \tag{10}$$

$$0 = R_r \bar{i}_r + \frac{d}{dt}\bar{\varphi}_r \tag{11}$$

$$\bar{\varphi}_s = L_s \bar{i}_s + M \bar{i}_r e^{jp\theta_1} \tag{12}$$

$$\bar{\varphi}_r = L_r \bar{i}_r + M \bar{i}_s e^{jp\theta_1} \tag{13}$$

$$C_e = \frac{pM}{L_r} \Im_m \left(\bar{i}_s . \bar{\varphi}_r^* \right) \tag{14}$$

Where * represents conjugated complex variables.
From Equation (14), we can write:

$$J \frac{d^2\theta_1}{dt^2} = \frac{pM}{L_r} \Im_m \left(\bar{i}_s . \bar{\varphi}_r^* \right) - C_r - f\dot{\theta} \tag{15}$$

We set (ρ) the modulus of the rotor flux and (δ) its position in the stationary reference frame (α, β), the rotor flux is defined as:

$$\bar{\varphi}_r = \rho e^{j\delta} \tag{16}$$

Figure 2. angle spotting

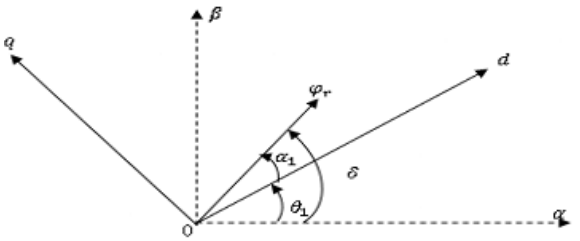

From Figure 2 we can write

$$\varphi_r = \bar{\varphi}_r e^{jp\theta_1} = \rho e^{j\alpha_1} \tag{17}$$

So we obtain:

$$\bar{i}_s = \frac{1}{M} \left(\bar{\varphi}_r + \frac{L_r}{R_r} \frac{d\bar{\varphi}_r}{dt} \right) \tag{18}$$

$$c_e = \frac{p}{R_r} \rho^2 \dot{\alpha}_1 \tag{19}$$

And from equation (15) we can define the following equation:

$$\rho = \sqrt{\frac{J.R\left(f\dot{\theta}_1 + \ddot{\theta}_1 + C_r\right)}{p\dot{\alpha}_1}} \tag{20}$$

Therefore

$$\tilde{\varphi}_r = \rho e^{j\alpha_1} = \mathcal{B}\left(\ddot{\theta}_1, \dot{\theta}_1, \alpha_1, \dot{\alpha}_1, C_r\right) \tag{21}$$

If we choose $y = \left(\alpha_1, \theta_1\right)$ as a flat output, we obtain then:

$$\tilde{\varphi}_r = \mathcal{B}\left(y, \dot{y}, \ddot{y}\right) \tag{22}$$

$$\tilde{i}_r = -\frac{1}{R_r}\frac{d}{dt}\overline{\varphi}_r = \mathbb{C}\left(\dot{\theta}_1, \ddot{\theta}_1, \theta_1^{(3)}, \dot{\alpha}_1, \ddot{\alpha}_1, C_r, \dot{C}_r\right) \tag{23}$$

$$\overline{i}_s = \frac{e^{jp\theta_1}}{M}\left(\overline{\varphi}_r - L_r\overline{i}_r\right) = \mathbb{C}\left(\dot{\theta}_1, \ddot{\theta}_1, \theta_1^{(3)}, \dot{\alpha}_1, \ddot{\alpha}_1, C_r, \dot{C}_r\right) \tag{24}$$

$$\overline{\varphi}_s = L_s\overline{i}_s + Me^{jp\theta_1}\overline{i}_r = \bullet\left(\dot{\theta}_1, \ddot{\theta}_1, \theta_1^{(3)}, \dot{\alpha}_1, \ddot{\alpha}_1, C_r, \dot{C}_r\right) \tag{25}$$

$$\overline{V}_s = R_s\overline{i}_s\frac{d}{dt}\overline{\varphi}_s = F\left(\dot{\theta}_1, \ddot{\theta}_1, \theta_1^{(3)}, \theta_1^{(4)}, \dot{\alpha}_1, \ddot{\alpha}_1, \alpha_1^{(3)}, C_r, \dot{C}_r, \ddot{C}_r\right) \tag{26}$$

we can say that the equations (17-26) satisfy the flatness conditions (2, 3, 4), so we can say that the induction motor is a differentially flat system.

3.2 Design of Flatness Control Based of IM

The mechanical model of the induction motor in the (*d –q)* reference frame is given by the following equations system:

$$\begin{cases} \dfrac{d\omega}{dt} = \dfrac{p}{JR_r}\rho\dfrac{M}{T_r}I_{sq} - \dfrac{\mathrm{f}}{\mathrm{J}}\omega - \dfrac{\mathrm{C_r}}{\mathrm{J}} \\ \dfrac{d\rho}{dt} = \dfrac{-1}{T_r}\rho + \dfrac{M}{T_r}I_{sd} \\ \dfrac{d\theta_1}{dt} = \omega \end{cases} \tag{27}$$

Where $\rho = \varphi_r = \varphi_{rd}$

Replace $(I_{sd}, I_{sq}, \rho, C_r)$ by $(I_{sd-ref}, I_{sq-ref}, \rho_{ref}, C_r)$, we obtain:

$$I_{sd-ref} = \frac{1}{M}\left(C_r\dot{\rho}_{ref} + \rho_{ref}\right) \tag{28}$$

$$I_{sq-ref} = \frac{L_r}{pM}\frac{J\ddot{\theta}_{1-ref} + f\dot{\theta}_{1-ref} + \hat{C}_r}{\rho_{ref}} \tag{29}$$

Where $\hat{C}_r$ it's the estimated load torque.

To estimate the load torque, we propose the following observer:

$$\begin{cases} \dfrac{d\hat{C}_r}{dt} = -l_1\left(\hat{\omega} - \omega\right) \\ \dfrac{d\hat{\omega}}{dt} = \dfrac{pM}{JL_r}\rho_{ref}I_{sq} - \dfrac{f}{J}\hat{\omega} - \dfrac{\hat{C}_r}{J} + l_2\left(\hat{\omega} - \omega\right) \end{cases} \tag{30}$$

Where: l_1 and l_2 are the observer gains.

The flux (ρ) and the estimated speed ($\hat{\omega}$) are obtained by the reduced order state observer (B Yassine, Fatiha, & Chrifi-Alaoui, 2020).

The dynamic error of the observer (30) is given by:

$$\frac{d}{dt}\begin{pmatrix}\epsilon_1 \\ \epsilon_2\end{pmatrix} = \begin{pmatrix} 0 & -l_1 \\ -\dfrac{1}{J} & -\dfrac{f}{J} + l_2 \end{pmatrix}\begin{pmatrix}\epsilon_1 \\ \epsilon_2\end{pmatrix} \tag{31}$$

Where: $\epsilon_1 = \hat{C}_r - C_r$ and $\epsilon_2 = \hat{\omega} - \omega$

The observer gain (30) is chosen in such a way that the dynamic error converges to zero. More details about the reduced order state observer applicable to the induction motor are given in (B Yassine et al., 2020)

Finally, the control of stator currents of the reduced model is to ensure by the PI regulators.

$$I_{sd}^{*} = k_{p\rho}\left(\hat{\rho} - \rho_{ref}\right) + k_{i\rho}\int_{0}^{t}\left(\hat{\rho} - \rho_{ref}\right)d\tau \tag{32}$$

$$I_{sq}^{*} = k_{p\omega}\left(\hat{\omega} - \omega_{ref}\right) + k_{i\omega}\int_{0}^{t}\left(\hat{\omega} - \omega_{ref}\right)d\tau \tag{33}$$

3.3 Planning Reference Trajectories

Applying the flatness approach, reference trajectories are defined by $(\rho_{ref}, \theta_{1-ref})$. The objective of this planning is:

- Respect the electromechanical constraints of the Induction motor.
- Guarantee the existence of bounded derivatives up to order two.

Therefore, the methodology chosen is to apply to the speed and flux set points a second-order filter making it possible to obtain the final reference trajectories that are derivable twice.

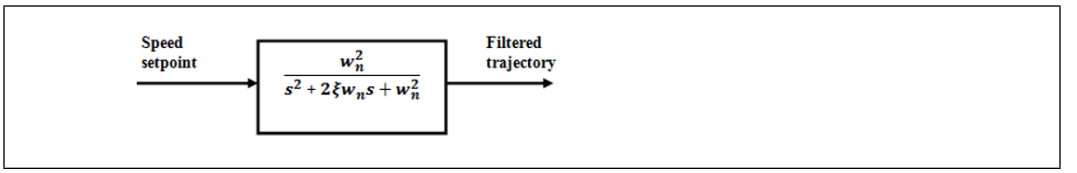

3.4 Complete Model Control

The proposed flatness-based control scheme with the use of reduced observer for estimation of the no measurable parameters of the motor's state vector is shown in Figure 3. Equations (10-11-12-13 and16) can be written as follows:

$$L_s\sigma\frac{d\bar{I}_s}{dt} = \bar{V}_s - R_s\bar{I}_s - \frac{M}{L_r}\left(\dot{\rho} + j\dot{\delta}\rho\right)e^{j\delta} \tag{34}$$

$$T_r\left(\dot{\rho} + j\dot{\alpha}_1\rho\right) = -\rho + Me^{-j\delta}\bar{I}_s \tag{35}$$

The nominal control planned voltages are defined as follows:

$$V_{sd}^{*} = \sigma L_s\left(\gamma I_{sd}^{**} - I_{sq}^{**}\frac{d\delta^{*}}{dt} + \frac{dI_{sd}^{**}}{dt} - \frac{M}{\sigma L_s L_r T_r}\rho_{ref}\right) \tag{36}$$

$$V_{sq}^{*} = \sigma L_{s}\left(\gamma I_{sq}^{**} + I_{sd}^{**}\frac{d\delta^{*}}{dt} + \frac{dI_{sq}^{**}}{dt} + \frac{M}{\sigma L_{s}L_{r}}p\omega^{*}\rho_{ref}\right) \tag{37}$$

Where: $\delta_{ref} = p\theta_{1-ref} + \int_{0}^{t}\dot{\alpha}_{1-ref}d\tau$

Currents I_{sd}^{**} and I_{sq}^{**} are given by:

$$I_{sd}^{**} = I_{sd}^{*} + k_{p\rho}\left(\hat{\rho} - \rho^{*}\right) + k_{i\rho}\int_{0}^{t}\left(\hat{\rho} - \rho^{*}\right)d\tau \tag{38}$$

$$I_{sq}^{**} = I_{sq}^{*} + k_{p\omega}\left(\hat{\rho} - \rho^{*}\right) + k_{i\omega}\int_{0}^{t}\left(\hat{\omega} - \omega^{*}\right)d\tau \tag{39}$$

From equations (38-39) and (27), we can write:

$$\frac{dI_{sd}^{**}}{dt} = \frac{dI_{sd-ref}}{dt} + \frac{T_{r}}{M}\begin{pmatrix} k_{i\rho}\left(\hat{\rho} - \rho_{ref}\right) \\ +k_{p\rho}\left(\frac{-\hat{\rho}}{T_{r}} + \frac{M}{T_{r}}I_{sd} - \dot{\rho}_{ref}\right)\end{pmatrix} \tag{40}$$

$$\frac{dI_{sq}^{**}}{dt} = \frac{dI_{sq}^{*}}{dt} + \frac{T_{r}}{M}\begin{pmatrix} k_{i\omega}\left(\hat{\omega} - \omega^{*}\right) + \\ k_{p\omega}\left(\frac{pM}{JL_{r}}\hat{\rho}I_{sq}^{**} - \frac{f}{J}\omega - \frac{\hat{C}_{r}}{J} - \dot{\omega}^{*}\right)\end{pmatrix} \tag{41}$$

Finally the control voltages are given by:

$$V_{sd} = V_{sd}^{*} + \sigma L_{s}\left(k_{pIsd}\left(I_{sd} - I_{sd}^{**}\right) + k_{iIsd}\int_{0}^{t}\left(I_{sd} - I_{sd}^{**}\right)d\tau\right) \tag{42}$$

$$V_{sq} = V_{sq}^{*} + \sigma L_{s}\left(k_{pIsq}\left(I_{sq} - I_{sq}^{**}\right) + k_{iIsq}\int_{0}^{t}\left(I_{sq} - I_{sq}^{**}\right)d\tau\right) \tag{43}$$

4. REDUCED MODEL REFERENCE ADAPTIVE SYSTEM OBSERVER

In this paper, a reduced MRAS observer is used to estimate the rotor speed and rotor flux (B Yassine et al., 2020). Fig .3 shows the block diagram of the reduced MRAS observe. From equation (10) and (11), we can deduce the following reduced model:

$$\begin{cases} \dfrac{d\varphi_{r\alpha}}{dt} = \dfrac{M}{T_r} i_{s\alpha} - \dfrac{1}{T_r}\varphi_{r\alpha} - \omega\varphi_{r\beta} \\ \dfrac{d\varphi_{r\beta}}{dt} = \dfrac{M}{T_r} i_{s\beta} - \dfrac{1}{T_r}\varphi_{r\beta} + \omega\varphi_{r\alpha} \end{cases} \tag{44}$$

If we replace ω by ω_{ref} while keeping $\varphi_{r\alpha}$ and $\varphi_{r\beta}$ as references, the system (44) becomes:

$$\begin{cases} \dfrac{d\varphi_{r\alpha}}{dt} = \dfrac{M}{T_r} i_{s\alpha} - \dfrac{1}{T_r}\varphi_{r\alpha} - \omega_{ref}\varphi_{r\beta} \\ \dfrac{d\varphi_{r\beta}}{dt} = \dfrac{M}{T_r} i_{s\beta} - \dfrac{1}{T_r}\varphi_{r\beta} + \omega_{ref}\varphi_{r\alpha} \end{cases} \tag{45}$$

If we now replace ω by $\hat{\omega}$, in this case the rotor flux $\varphi_{r\alpha}$ and $\varphi_{r\beta}$ are considered as estimated values, the model (44) becomes:

$$\begin{cases} \dfrac{d\hat{\varphi}_{r\alpha}}{dt} = \dfrac{M}{T_r} i_{s\alpha} - \dfrac{1}{T_r}\hat{\varphi}_{r\alpha} - \hat{\omega}\hat{\varphi}_{r\beta} \\ \dfrac{d\hat{\varphi}_{r\beta}}{dt} = \dfrac{M}{T_r} i_{s\beta} - \dfrac{1}{T_r}\hat{\varphi}_{r\beta} + \hat{\omega}\hat{\varphi}_{r\alpha} \end{cases} \tag{46}$$

With the equations (45) and (46), we can establish the following error dynamics:

$$e = \begin{bmatrix} e_{r\alpha} \\ e_{r\beta} \end{bmatrix} = \begin{bmatrix} \varphi_{r\alpha} - \hat{\varphi}_{r\alpha} \\ \varphi_{r\beta} - \hat{\varphi}_{r\beta} \end{bmatrix} \tag{47}$$

The error e can be written in the following complex form:

$$\overline{e} = e_{r\alpha} + j e_{r\beta} \tag{48}$$

And the system (45) can be written in following complex form:

$$\frac{M}{T_r}\overline{i}_s = \frac{d\overline{\varphi}_r}{dt} + \frac{\overline{\varphi}_r}{T_r} - j\omega\overline{\varphi}_r \tag{49}$$

for $\omega = \omega_{ref}$, we will have:

$$\frac{M}{T_r}\overline{i}_s = \frac{d\overline{\varphi}_r}{dt} + \frac{\overline{\varphi}_r}{T_r} - j\omega_{ref}\overline{\varphi}_r \tag{50}$$

for $\omega = \hat{\omega}$, we will have:

$$\frac{M}{T_r}\hat{\overline{i}}_s = \frac{d\hat{\overline{\varphi}}_r}{dt} + \frac{\hat{\overline{\varphi}}_r}{T_r} - j\hat{\omega}\hat{\overline{\varphi}}_r \tag{51}$$

Let us make now the subtraction between (51) and (50), we can write:

$$0 = \dot{\overline{e}} + \frac{1}{T_r}\overline{e} - j\omega_{ref}\overline{\varphi}_r + j\hat{\omega}\hat{\overline{\varphi}}_r = \dot{\overline{e}} + \frac{1}{T_r}\overline{e} - j\omega_{ref}\overline{\varphi}_r + j\hat{\omega}\hat{\overline{\varphi}}_r + j\omega_{ref}\hat{\overline{\varphi}}_r - j\omega_{ref}\hat{\overline{\varphi}}_r$$

$$= \dot{\overline{e}} + \left(\frac{1}{T_r} - j\omega_{ref}\right)\overline{e} - j\left(\omega_{ref} - \hat{\omega}\right)\hat{\overline{\varphi}}_r \tag{52}$$

This gives:

$$\dot{\overline{e}} = \overline{A}\,\overline{e} + \overline{W} \tag{53}$$

Where: $\overline{A} = -\left(\frac{1}{T_r} - j\omega_{ref}\right)$

With: $A = \begin{bmatrix} -\frac{1}{T_r} & -\omega_{ref} \\ \omega_{ref} & -\frac{1}{T_r} \end{bmatrix}$

and:

$$\overline{W} = j\left(\omega_{ref} - \hat{\omega}\right)\hat{\overline{\varphi}}_r \tag{54}$$

$$W = \Delta\omega \begin{bmatrix} 0 & -1 \\ 1 & 0 \end{bmatrix} \begin{bmatrix} \hat{\varphi}_{r\alpha} \\ \hat{\varphi}_{r\beta} \end{bmatrix} \tag{55}$$

The stability of algorithm (53) is studied using the hyper-stability Popov criterion. To do, we define the following Lyapunov function:

$$V = e^T e + \frac{\left(\omega_{ref} - \hat{\omega}\right)^2}{2\gamma} \geq 0 \tag{56}$$

Where: γ is a positive constant.
The function given in (56) is globally negative definite. Thus, $\dot{V} < 0 \quad \forall\ \hat{\omega}$

The time derivative of the Lyapunov function becomes:

$$\dot{V} = \frac{1}{2}\left(\dot{e}^T e + e^T \dot{e}\right) + \frac{1}{\gamma}\Delta\omega \frac{d\left(\Delta\omega\right)}{dt} + \frac{e_\omega^2}{2}$$

Let us replace $\dot{e}$ by its value:

$$\dot{V} = \frac{1}{2}\left(\left(Ae + \bar{W}\right)^T .e + e^T\left(Ae + \bar{W}\right)\right) + \frac{\Delta\omega}{\gamma}\frac{d\left(\Delta\omega\right)}{dt}$$

$$= \frac{1}{2}\left(e^T A^T e + \bar{W}^T e + e^T Ae + e^T \bar{W}\right) + \frac{\Delta\omega}{\gamma}\frac{d\left(\Delta\omega\right)}{dt}$$

$$\dot{V} = \frac{1}{2}\left(e^T\left(A^T + A\right)e\right) + e^T\bar{W} + \frac{\Delta\omega}{\gamma}\frac{d\left(\Delta\omega\right)}{dt} + \frac{de_\omega}{dt}e_\omega = Q + P \tag{57}$$

where:

$$Q = \frac{1}{2}\left(A^T + A\right) = \frac{1}{2}\left(\begin{bmatrix} -\frac{1}{T_r} & -\omega_{ref} \\ \omega_{ref} & -\frac{1}{T_r} \end{bmatrix} + \begin{bmatrix} -\frac{1}{T_r} & \omega_{ref} \\ -\omega_{ref} & -\frac{1}{T_r} \end{bmatrix}\right)$$

$$= \frac{-1}{T_r}\begin{bmatrix} 1 & 0 \\ 0 & 1 \end{bmatrix} < 0$$

The first term of (57) is negative, If $P = 0$ then:

$$e^T\bar{W} = -\frac{\Delta\omega}{\gamma}\frac{d\left(\Delta\omega\right)}{dt} \tag{58}$$

Where:

$$e^T\bar{W} = \Delta\omega\left[\varphi_{r\alpha} - \hat{\varphi}_{r\alpha} \quad \varphi_{r\beta} - \hat{\varphi}_{r\beta}\right].\begin{bmatrix} \hat{\varphi}_{r\beta} \\ -\hat{\varphi}_{r\alpha} \end{bmatrix} = \Delta\omega\left(\varphi_{r\alpha}\hat{\varphi}_{r\beta} - \varphi_{r\beta}\hat{\varphi}_{r\alpha}\right) \tag{59}$$

We Replace (59) into (58), we obtain:

$$\frac{d\hat{\omega}}{dt} = \gamma\left(\varphi_{r\alpha}\hat{\varphi}_{r\beta} - \varphi_{r\beta}\hat{\varphi}_{r\alpha}\right)$$

$$\hat{\omega} = \gamma\int\left(\varphi_{r\alpha}\hat{\varphi}_{r\beta} - \varphi_{r\beta}\hat{\varphi}_{r\alpha}\right)dt \tag{60}$$

it should be noted that, to improve the precision amounts adding a proportional gain to the integral action (K_p, K_i).

$$\hat{\omega} = K_p\left(\varphi_{r\alpha}\hat{\varphi}_{r\beta} - \varphi_{r\beta}\hat{\varphi}_{r\alpha}\right) + K_i\int\left(\varphi_{r\alpha}\hat{\varphi}_{r\beta} - \varphi_{r\beta}\hat{\varphi}_{r\alpha}\right)dt\ . \tag{61}$$

Figure 3. Bloc diagram of reduced-order state observer.

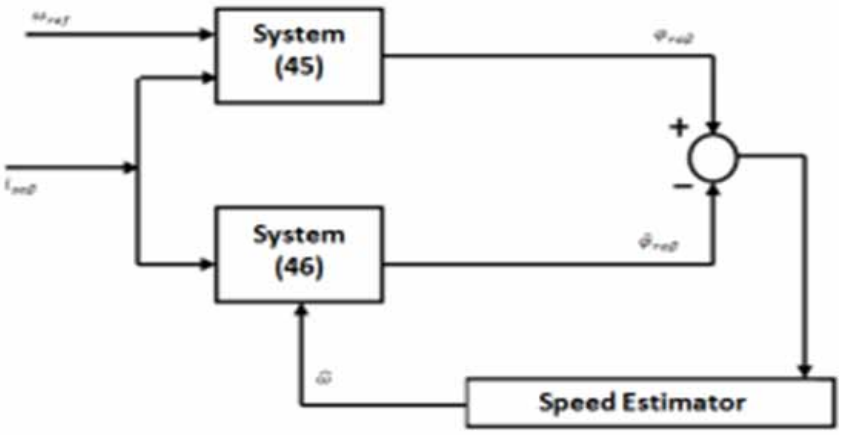

Figure 4. Schematic diagram the proposed flatness-based control scheme with the use of reduced observer

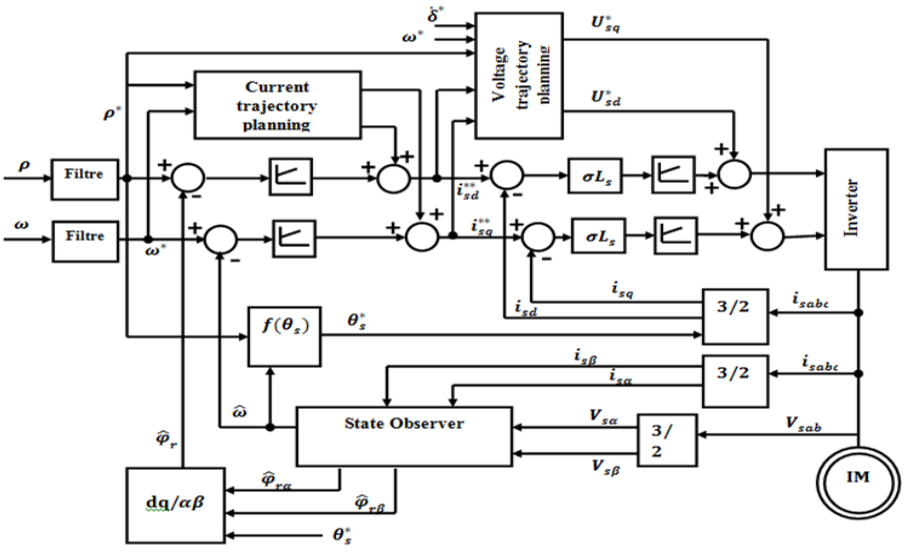

5. SIMULATION AND EXPERIMENTAL RESULTS

The proposed sensorless control is simulated under the Matlab/Simulink environment. The motor parameters are: $R_r = 4.2\ \Omega$; Rs =5.72 Ω ; Ls= 0.462 H; L_r= 0.462 H; M =0.44 H; J= 0.0049 Kgm^2; f= 0.003 Nm.s/rad; P =2; the motor power is 1.5 Kw.

The simulation results are shown in Figure 5. The figure 5a shows that the estimated speed follows the reference, despite the application of load (1,5 Nm), the estimated speed always follows the speed reference.

We can see in Figure 5c that the flux ($\hat{\varphi}_{r\alpha\beta}$) installs correctly and well sinusoidal.

The test bench used for the experimental validation of proposed control is shown In Figure 8. The sampling frequency is fixed at 10 kHz and the controller receives the stator currents measurements through two 8- bit A/D converters. Then, using the PWM technique, the reference voltages are sent to the machine via the voltage-source inverter whose switching frequency is fixed at 10 kHz.

Figure 7 shows the experimental results obtained for the proposed sensorless control by differential flatness method. A rotor speed reference is imposed with a load torque equal to 1.5 Nm applied at time t = 4.2 s.

By comparing the results (simulation and experimental), we can see that both results are very similar. It will be noticed that the estimated and the real rotor speed signals are very close. Finally, we can say that the results confirm the validity of the proposed control. According to the results we can say that the speed response obtained by the flatness technique is significantly improved compared to that obtained by the classical sensorless vector control shows in Figure 8.

Figure 5a. Simulation result of Rotor Speed.

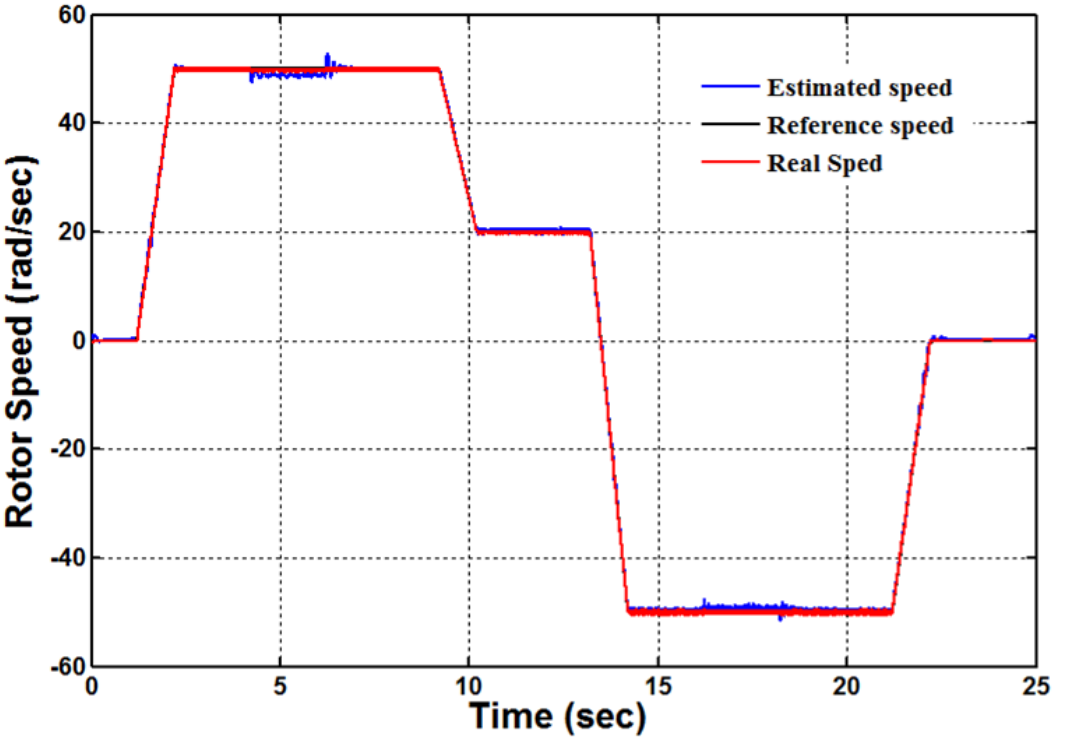

Figure 5b. Simulation result of Rotor Speed (Zoom).

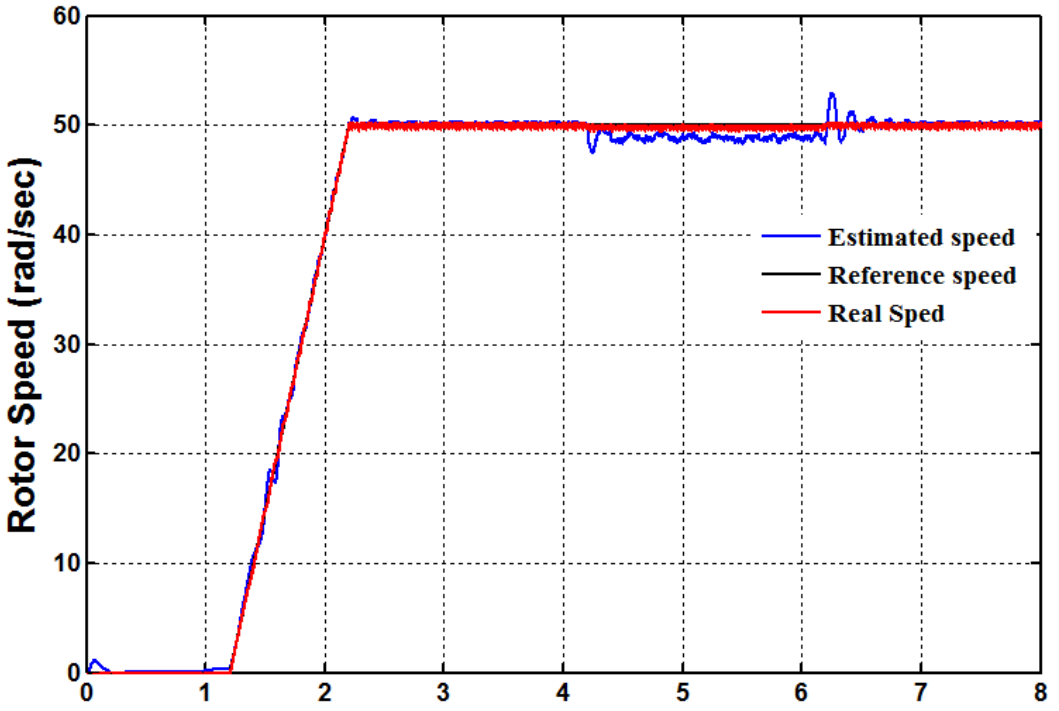

Figure 5c. Simulation result of Estimated Rotor Flux.

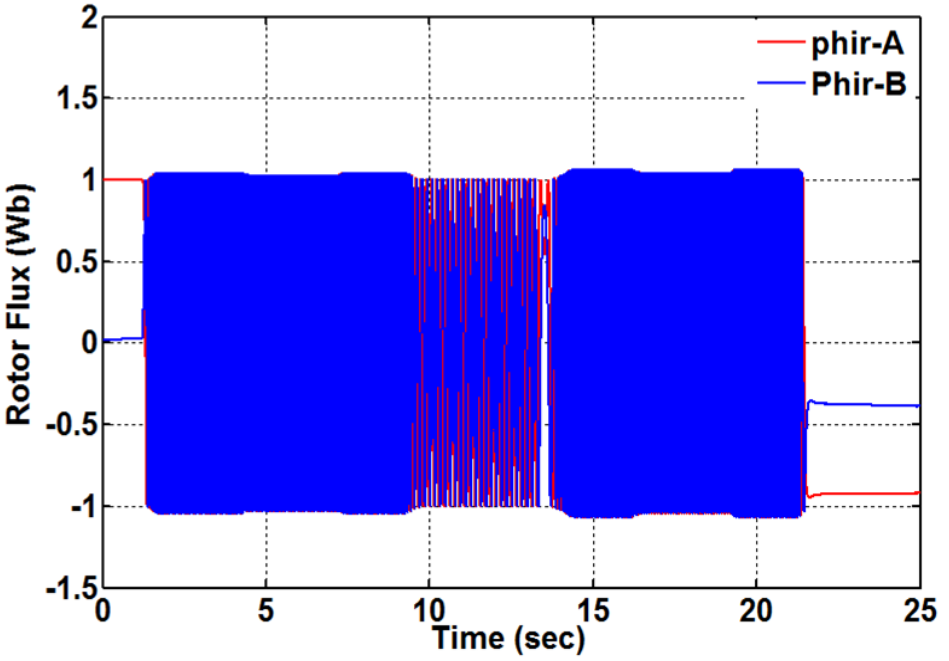

Figure 5d. Simulation result of Estimated Rotor Flux (Zoom).

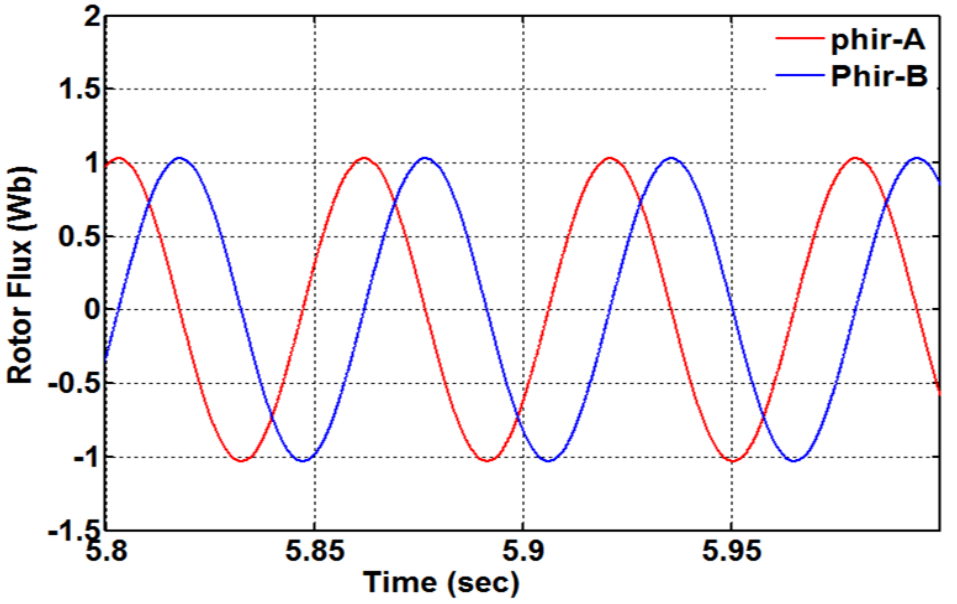

Figure 6a. Experimental result of Rotor Speed.

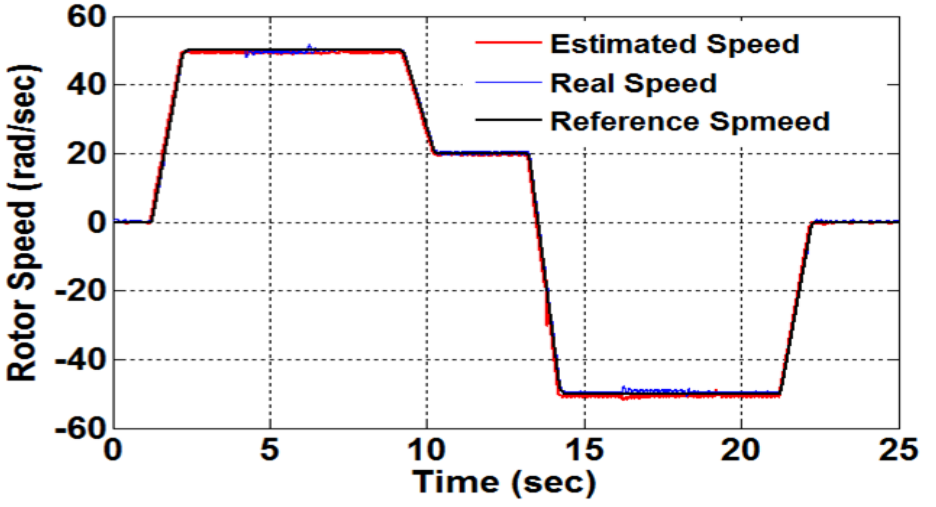

Figure 6b. Experimental result of Rotor Speed (Zoom).

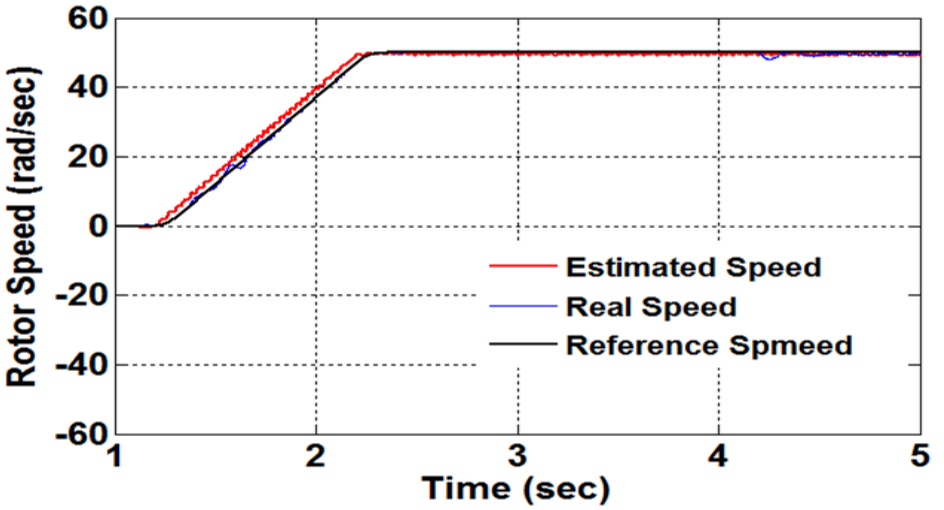

Figure 6c. Experimental result of Estimated Rotor Flux.

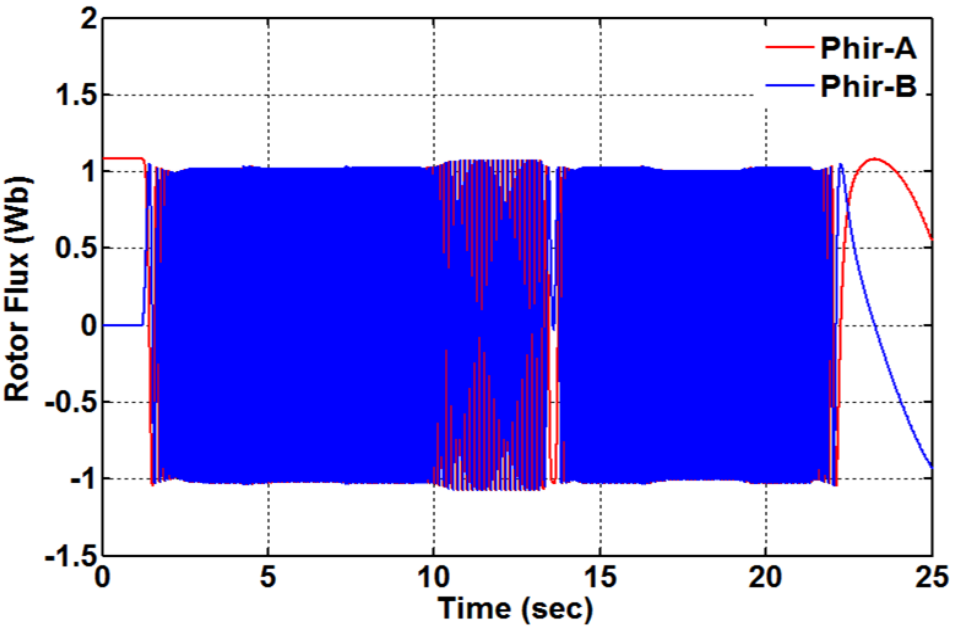

Figure 6d. Experimental result of Estimated Rotor Flux (Zoom).

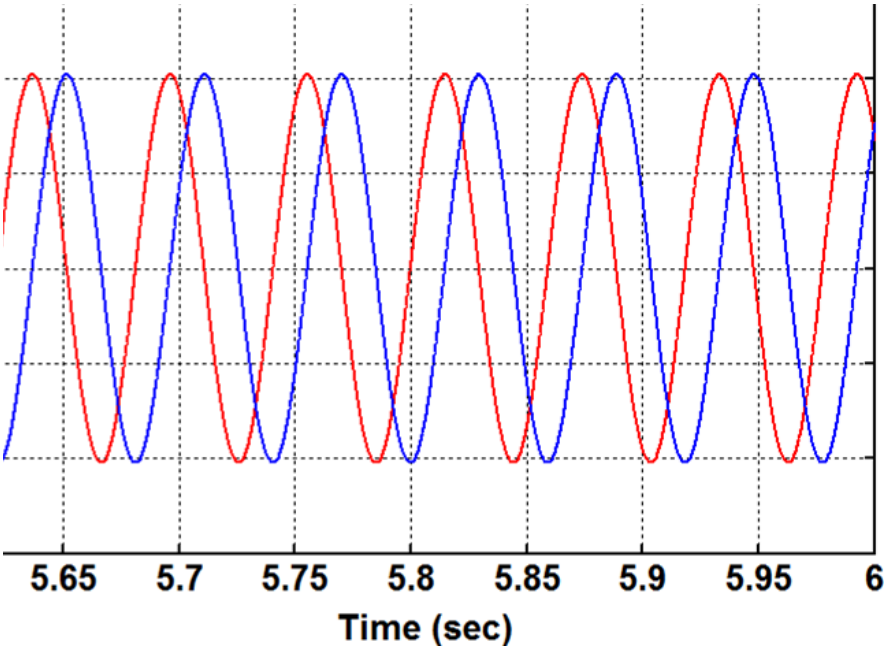

Figure 7a. Experimental result of Rotor Speed (classical FOC).

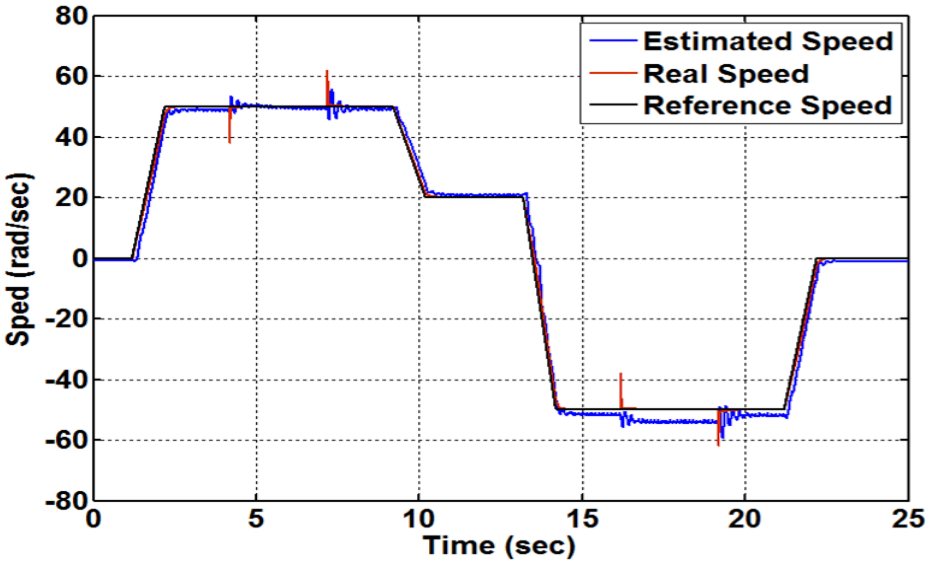

Figure 7b. Experimental result of Rotor Speed (classical FOC), Zoom..

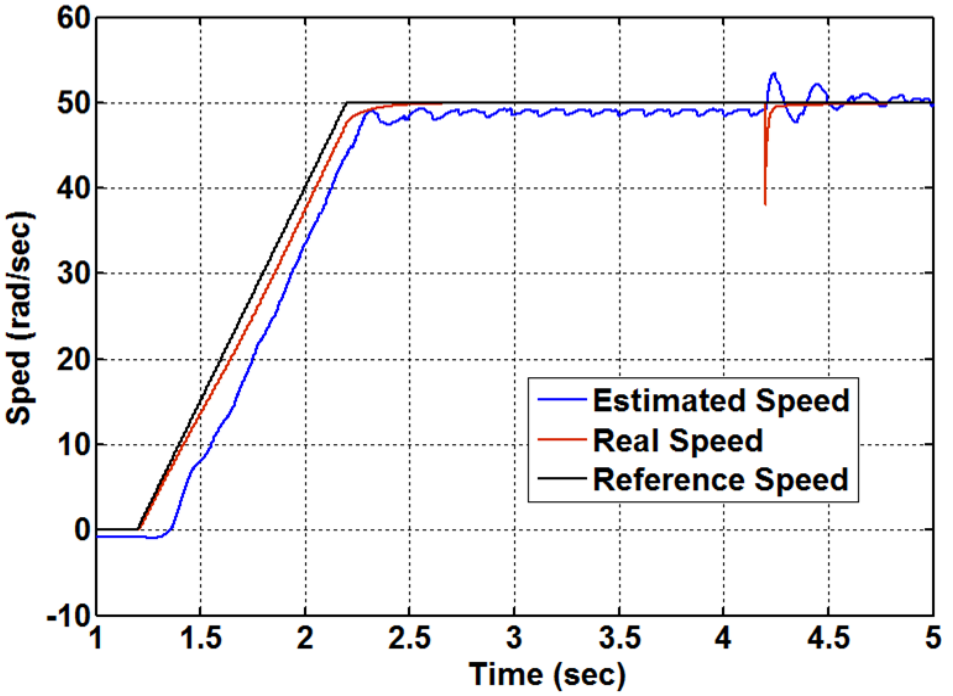

Figure 7c. Experimental result of Estimated Rotor Flux (classical FOC), .

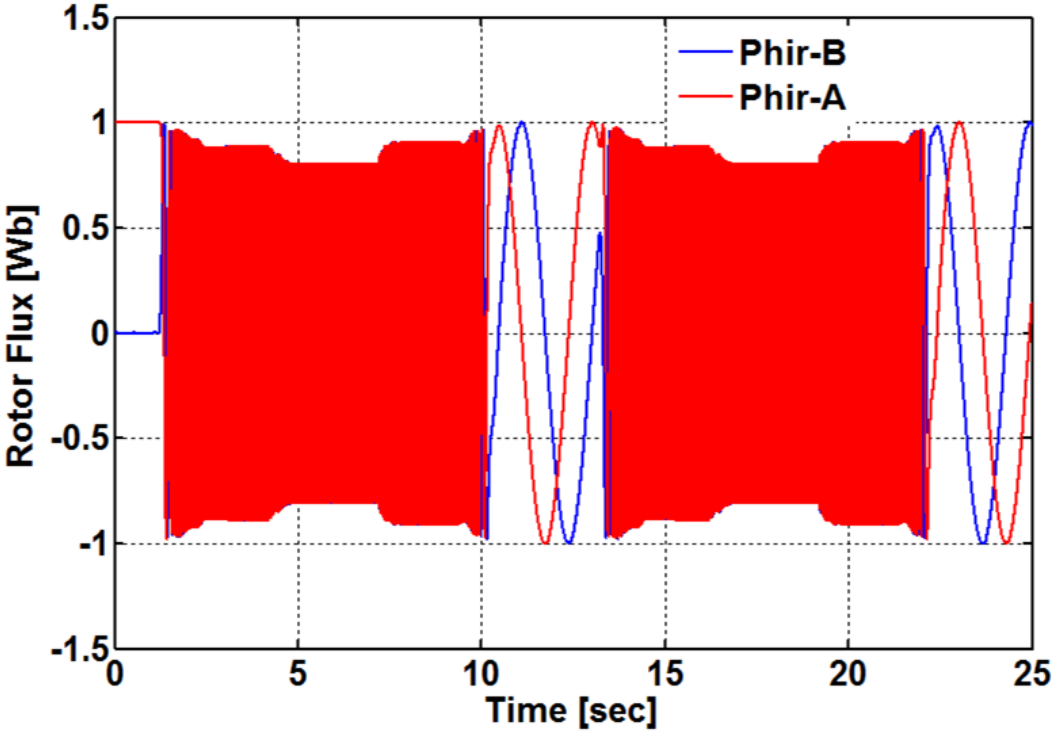

Figure 8. Experimental result of Estimated Rotor Flux (classical FOC), Zoom.

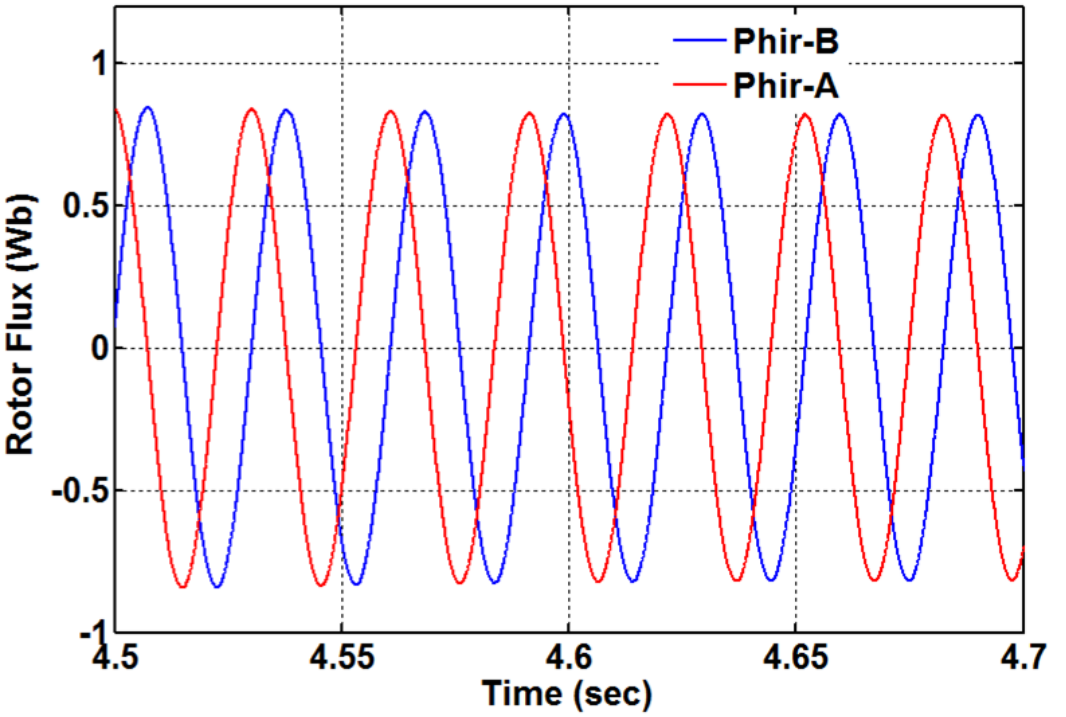

Figure 9. The photograph of the experimental test system.

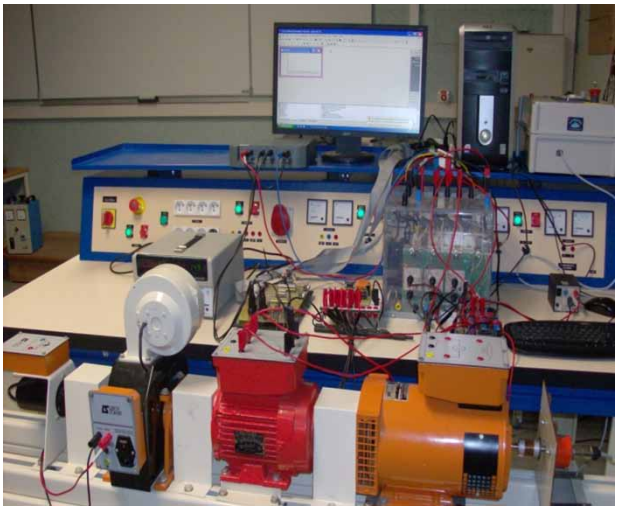

6. CONCLUSION

In This paper, Authors have studied the sensorless control for induction motors using differential flatness theory and reduced MRAS observer.

The experimental results have shown that an adequate sensorless speed control by differential flatness method of IM drive can be achieved at rated, low, and zero reference speed control. Obtained results show that this control strategy assures a perfect linearization regardless trajectory profiles physically imposed on the induction machine. Despite the test at very low speed, the reduced MRAS observer is functioning normally. Finally the proposed control has given very satisfactory results in terms of load disturbance rejection and tracking rotor speed.

REFERENCES

Abdollahi, R. (2021). Induction motor drive based on direct torque controlled used multi-pulse AC-DC rectifier. *International Journal of Applied*, *10*(2), 89–96. doi:10.11591/ijape.v10.i2.pp89-96

Adamczyk, M., & Orlowska-Kowalska, T. (2021). Post-Fault Direct Field-Oriented Control of Induction Motor Drive using Adaptive Virtual Current Sensor. *IEEE Transactions on Industrial Electronics*, 1. doi:10.1109/TIE.2021.3075863

Al-Rouh, I. (2004). *Contribution à la commande sans capteur de la machine asynchrone.* Université Henri Poincaré-Nancy 1.

Armando, E., Boglietti, A., Musumeci, S., & Rubino, S. (2021). Flux-Decay Test: A Viable Solution to Evaluate the Induction Motor Rotor Time-Constant. *IEEE Transactions on Industry Applications*, *57*(4), 3619–3631. doi:10.1109/TIA.2021.3076425

Chang, G.-W., Espinosa-Perez, G., Mendes, E., & Ortega, R. (2000). Tuning rules for the PI gains of field-oriented controllers of induction motors. *IEEE Transactions on Industrial Electronics*, *47*(3), 592–602. doi:10.1109/41.847900

Comanescu, M. (2016). Design and implementation of a highly robust sensorless sliding mode observer for the flux magnitude of the induction motor. *IEEE Transactions on Energy Conversion*, *31*(2), 649–657. doi:10.1109/TEC.2016.2516951

Dannehl, J., & Fuchs, F. W. (2006). *Flatness-based control of an induction machine fed via voltage source inverter-concept, control design and performance analysis.* Paper presented at the IECON 2006-32nd annual conference on IEEE industrial electronics. doi:10.1109/IECON.2006.347840

De Doncker, R. W., & Novotny, D. W. (1994). The universal field oriented controller. *IEEE Transactions on Industry Applications*, *30*(1), 92–100. doi:10.1109/28.273626

De Wit, P. A., Ortega, R., & Mareels, I. (1996). Indirect field-oriented control of induction motors is robustly globally stable. *Automatica*, *32*(10), 1393–1402. doi:10.1016/0005-1098(96)00070-2

Enany, T., Wahba, W., & Hassan, M. M. (2014). A Remote and Sensorless Stator Winding Temperature Estimation Method for Thermal Protection for Induction Motor. *International Journal of System Dynamics Applications*, *3*(3), 53–72. doi:10.4018/ijsda.2014070103

Fliess, M., Lévine, J., Martin, P., & Rouchon, P. (1995). Flatness and defect of non-linear systems: Introductory theory and examples. *International Journal of Control*, *61*(6), 1327–1361. doi:10.1080/00207179508921959

Fliess, M., Lévine, J., Martin, P., & Rouchon, P. (1999). A lie-backlund approach to equivalence and flatness of nonlinear systems. *IEEE Transactions on Automatic Control*, *44*(5), 922–937. doi:10.1109/9.763209

Ha, V. T., & Quang, N. P. (2019). *Flatness-Based Control Design for Two-Mass System Using Induction.* Paper presented at the Engineer of the XXI Century: Proceedings of the VIII International Conference of Students, PhD Students and Young Scientists.

Ha, V. T., & Quang, N. P. (2020). *Flatness-Based Control Design for Two-Mass System Using Induction Motor Drive Fed by Voltage Source Inverter with Ideal Control Performance of Stator Current. In Engineer of the XXI Century*. Springer. doi:10.1007/978-3-030-13321-4_4

Hussein, H. T., Ammar, M., & Hassan, M. M. (2017). Three phase induction motor's stator turns fault analysis based on artificial intelligence. *International Journal of System Dynamics Applications*, *6*(3), 1–19. doi:10.4018/IJSDA.2017070101

Ismail, M. M. (2012). Applications of anfis and fuzzy algorithms for improvement of the DTC performance for the three phase saturated model of induction motor. *International Journal of System Dynamics Applications*, *1*(3), 54–83. doi:10.4018/ijsda.2012070102

Lorenz, R. D., Lipo, T. A., & Novotny, D. W. (1994). Motion control with induction motors. *Proceedings of the IEEE*, *82*(8), 1215–1240. doi:10.1109/5.301685

Manceur, M. (2012). Commande robuste des systèmes non linéaires complexes. Academic Press.

Morand, F. (2005). *Techniques d'observation sans capteur de vitesse en vue de la commande des machines asynchrones*. Academic Press.

Mustafa, M. O., Nikolakopoulos, G., & Gustafsson, T. (2014). Faults Classification Scheme for Three Phase Induction Motor. *International Journal of System Dynamics Applications*, *3*(1), 1–20. doi:10.4018/ijsda.2014010101

Nazemi, M. H., Gallehdar, D., Haghjoo, F., & Cruz, S. (2021). A secure and sensitive wavelet transform based technique for stator fault detection in the cases of line-connected and inverter-fed induction machines. *IET Electric Power Applications*, *15*(9), 1138–1153. doi:10.1049/elp2.12084

Salima, M., Loubna, A., & Riad, T. (2018). A global stability of linearizing control of induction motor for PV water pumping application. *International Journal of System Dynamics Applications*, *7*(3), 31–56. doi:10.4018/IJSDA.2018070102

Savarapu, S., & Narri, Y. (n.d.). Real-Time Implementation of Brain Emotional Controller for Sensorless Induction Motor Drive with Adaptive System. *Modern Approaches in Machine Learning and Cognitive Science: A Walkthrough: Latest Trends in AI, 2*, 95.

Vasu, K., Thalluru, M. K., & Kumar, A. (2021). Improved Performance of Photovoltaic Array for Water Pumping by Fuzzy Control in Sensorless Vector Control of Induction Motor Drive. *International Journal of Ambient Energy*, 1-15.

Yassine, B., Fatiha, Z., & Chrifi-Alaoui, L. (2020). IS-MRAS With On-Line Adaptation Parameters Based on Type-2 Fuzzy LOGIC for Sensorless Control of IM. *Iranian Journal of Electrical and Electronic Engineering*, *16*(1), 85–95.

Zbede, Y. B., Gadoue, S. M., & Atkinson, D. J. (2016). Model predictive MRAS estimator for sensorless induction motor drives. *IEEE Transactions on Industrial Electronics*, *63*(6), 3511–3521. doi:10.1109/TIE.2016.2521721